The 9th European Congress on Computational Methods in Applied Sciences and Engineering
ECCOMAS Congress 2024
3–7 June 2024, Lisboa, Portugal

EFFECT OF THE CAROTID GEOMETRY ON THE ONSET OF ATHEROSCLEROTIC PLAQUES

MARIA VITTORIA SALVETTI[1], JASKARAN SINGH[1], KATIA CAPELLINI[2], ALESSANDRO MARIOTTI[1] AND SIMONA CELI[2]

[1] Department of Civil and Industrial Engineering, University of Pisa
Largo Lucio Lazzarino, 2, 56122 Pisa, Italy
e-mail: maria.vittoria.salvetti@unipi.it

[2] BioCardioLab - Heart Hospital, Fondazione Toscana G. Monasterio
Via Aurelia Sud, 54100 Massa, Italy

Key words: Computational Fluid Dynamics, hemodynamic simulations, atherosclerotic plaques, carotid arteries, stochastic sensitivity analysis.

Summary. Atherosclerosis is an inflammatory cardiovascular disease characterized by the formation of plaques inside arteries. These plaques result from the accumulation of lipidic substances over the years and can obstruct blood flow to downstream vessels and organs. Our objective is to predict the possible onset of carotid plaques using Computational Fluid Dynamics (CFD) simulations and to analyze the influence of hemodynamic and geometric parameters on the early stages of the disease through stochastic sensitivity analysis. The ultimate goal is to determine whether geometric parameters can be considered risk factors.

We combine CFD simulations with a model for predicting plaque onset and growth in the carotid arteries. In this model, plaque growth depends on CFD-predicted wall shear stresses and the concentration and accumulation of Low-Density Lipoprotein (LDL) in the vessel. Low values of wall shear stress and higher LDL concentrations promote plaque formation. Starting with a clinical dataset that includes 3D segmented geometries of the right and left carotids, as well as flow rate waveforms in the common, external, and internal carotid arteries (CCA, ECA, and ICA), we construct a parametric geometry to identify which geometric parameters describing the carotid bifurcation are primarily responsible for the possible onset and growth of arteriosclerotic plaques. Continuous response surfaces of plaque growth in the geometrical parameter space are obtained using a probabilistic framework based on stochastic collocation methods and sparsification.

Results indicate that the position of the ICA inflection point significantly impacts the location and extent of the plaque. The Reynolds number also plays a role in plaque development, as it directly affects the magnitude of wall shear stresses.

1 INTRODUCTION

Atherosclerosis is a cardiovascular disease (CVD) that gradually narrows the arteries due to the formation of plaques in medium and large-sized blood vessels [1, 2]. This can obstruct the blood supply to downstream vessels and organs, making it one of the major causes of death in Western countries over the last few decades [3], accounting for 31.5% of all global deaths [4]

for cardiovascular disease. Therefore, it is crucial to understand the genesis of atherosclerotic plaques by identifying the main risk factors [5].

Computational Fluid Dynamics (CFD) simulations integrated with in-vivo data and disease-specific mathematical models have been frequently used to analyze hemodynamic blood flows, predict pathology evolution, and assess associated risks [6, 7]. Various mathematical models specific to the carotid arteries have been developed to predict atherosclerotic plaque onset and growth, as reviewed in [8]. Simple models consider linear relationships between wall displacement and fluid-dynamic variables, such as the Wall Shear Stress (WSS) model [9], whereas more complex models include additional parameters, like the Low-Density Lipoprotein (LDL) model in [10], or describe the complete biological process using ordinary differential equations [11]. These models have been applied to either simple 2D/3D geometries [12] or more realistic patient-specific 3D models [7] and boundary conditions [13, 14].

The arterial wall can be considered rigid or deformable for fluid-structure interaction and can be modeled as a single layer of endothelial cells [10] or as a porous multi-layer vessel structure [15]. Blood is modeled as a Newtonian fluid in large vessels [7, 16], while in smaller vessels such as the carotids, non-Newtonian blood rheology is frequently employed to capture the shear-thinning effect near the walls [17, 18], which directly influences the distribution of WSS sensed by endothelial cells and consequently the prediction of plaque growth.

Among the possible risk factors, the geometrical parameters influence the hemodynamics of blood flow, prompting some parametric and Uncertainty Quantification studies to consider the influence of carotid geometrical features on plaque growth [19, 20, 21]. A large carotid sinus and an increasing bifurcation angle promote low and oscillating wall shear stress (WSS) and reverse flow [22], as do high values of the proximal area ratio [23]. This leads to a higher propensity for plaque formation. Conversely, a larger carotid tortuosity is often associated with higher WSS values [23] and a reduced risk of plaque onset. Additionally, the inlet and outlet diameters of the carotid and the out-of-plane curvature of the branches influence the hemodynamics in the branching region [20]. Low velocity values near the walls again promote plaque formation.

In this study, we conduct a stochastic sensitivity analysis to assess which geometric parameters of the carotid geometry most impact plaque onset and growth. We carried out numerical simulations coupled with the plaque growth model from Gessaghi et al. [10]. We derive the parametric geometry of the carotids and the flow-rate waveform from an in-vivo acquired dataset by locally modifying the geometry in the bifurcation region. We conduct an Uncertainty Quantification (UQ) analysis using a stochastic collocation method with sparse grids to build continuous response surfaces in the parameter space and to highlight how the risk factor is influenced by geometrical parameters

2 MATERIALS AND METHODS

2.1 Clinical data-set and parametric geometry

The patient-specific clinical dataset of a 78-year-old male subject was obtained through in-vivo measurements with his written consent. It contains (i) patient-specific diseased right and left carotid images acquired from Computed Tomography (CT scan) and (ii) inlet/outlet flow rates obtained from 4D-flow Magnetic Resonance Imaging (4D-flow MRI).

The diseased carotid geometric models are segmented from CT scans, and the healthy geometric models are derived from the diseased models by applying an idealized endarterectomy.

The patient-specific right and left carotids are used as references for constructing the parametric carotid geometries. First, the original layout of the spline describing the ICA and ECA is determined, as shown by the black line in Figure 1a for the right carotid and Figure 1b for the left carotid. Then, these reference models are modified in the bifurcation region of the carotids, on both the Internal Carotid Artery (ICA) and the External Carotid Artery (ECA) sides. The modified geometries are obtained by varying the spline based on the chosen uncertain geometrical parameters − ECA inflection point, ICA inflection point, ECA spline curvature, ICA spline curvature, and the Reynolds number − within a defined interval range. A possible parametric geometry is shown in Figure 1a for the right carotid and in Figure 1b for the left carotid, where the modified spline layout is highlighted in red, overlapped on the original layout in black. The range of variation is determined to ensure physiologically realistic carotid parametric geometries.

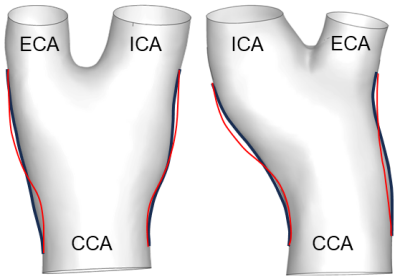

Figure 1: Sketch of the (a) right and (b) left patient-specific carotid geometrical models (black lines) and example of parametric splines (red lines).

The 4D-flow MRI data are interpolated over the cardiac cycle period of T = 0.8 s to match the flow rate waveforms at the Common Carotid Artery (CCA), ICA, and ECA, as shown in Figure 2a and Figure 2c for the right carotid, and in Figure 2b and Figure 2d for the left carotid.

2.2 Numerical methodology and boundary conditions

The blood flow in the 3D fluid domain, Ω, represented by the healthy carotid lumen, is solved numerically by discretizing the Navier-Stokes continuity and momentum equations in the steady incompressible form:

$$\begin{aligned} \nabla \cdot \mathbf{v} &= \mathbf{0} \quad \mathbf{x} \in \Omega \\ \rho(\mathbf{v} \cdot \nabla)\mathbf{v} + \nabla p - \mu \Delta \mathbf{v} &= \mathbf{0} \quad \mathbf{x} \in \Omega \end{aligned} \tag{1}$$

where $\mathbf{v}$ represents the velocity flow field and p represents the pressure divided by the density. In our case, the blood has a constant density $\rho = 1050$ kg/m^3.

We carry out laminar simulations using a commercial finite-volume solver. Indeed, the Reynolds number based on the bulk velocity and carotid diameter is always below 300. The segregated SIMPLE algorithm is employed together with second-order-accurate spatial discretization schemes. The blood is considered non-Newtonian with a shear-rate-dependent molecular viscosity, η, described through the Carreau-Yasuda model [17]. The non-Newtonian model allows to capture the shear-thinning effect, which causes a viscosity decrease with an increased shear rate near the arterial wall, that is intricately connected to the microscopic structure of blood

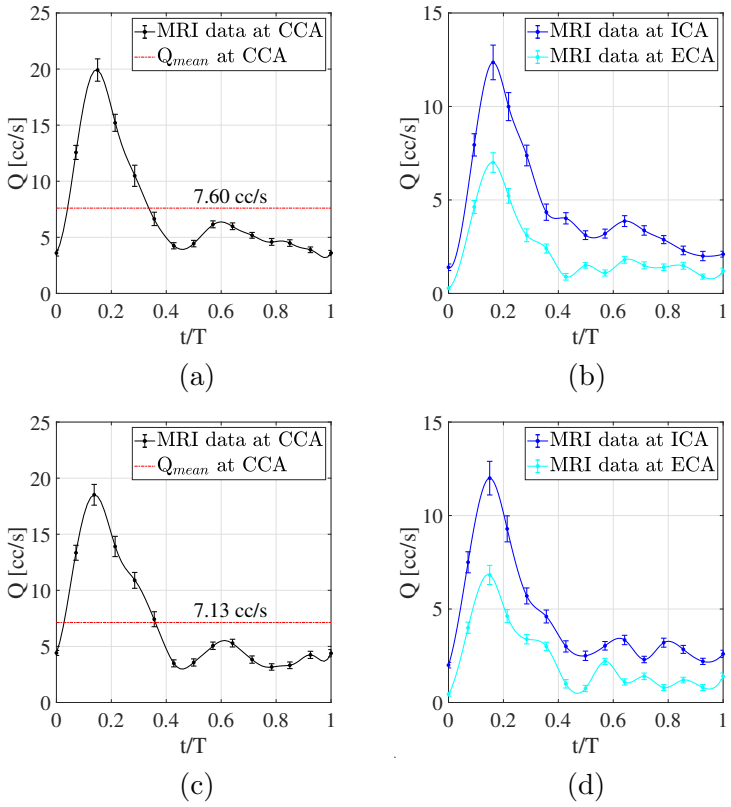

Figure 2: *In-vivo*-acquired flow-rate waveforms for (a,b) right carotid and (c,d) left carotid. Cardiac-cycle averaged values are also reported.

and provides a more precise evaluation of the low and oscillating WSS in complex flow patterns regions [18].

As concern the boundary conditions, fully-developed cardiac-cycle-averaged velocity profile is imposed at the CCA inlets. Inlet flow-rate waveforms and the cycle-averaged value are shown in Figs 2(a) and 2(b) for the right and left CCAs, respectively. A flow split ratio condition is imposed at the ICA and ECA outlet sections to match clinical data: $Q_{ICA} = 0.66 Q_{CCA}$ and $Q_{ECA} = 0.34 Q_{CCA}$ for the right carotid and $Q_{ICA} = 0.61 Q_{CCA}$ and $Q_{ECA} = 0.39 Q_{CCA}$ for the left carotid. The operating pressure is set at 93.3 mmHg. The artery walls are considered rigid, impermeable, with no-slip conditions. The fluid domain Ω is discretized through a polyhedric computational grid with a prism layer at the wall. After grid independence analysis, a grid of about $4 \cdot 10^5$ nodes is used for each carotid.

2.3 Plaque-growth model and morphing procedure

We apply the model developed in [10] to predict the early stages of atherosclerotic plaque onset and growth in patient-specific carotids. The arterial wall displacement is related to the magnitude of the wall shear stress τ, the concentration and transport of the LDL in the vessel lumen, the LDL passage through the vessel wall into the intima where it accumulates and oxidizes, and other hemodynamic variables. Given the CFD-computed velocity and τ fields, the

wall displacement representing plaque growth is evaluated through coupled first-order ordinary differential equations:

$$\begin{aligned} \dot{\mathrm{m}} &= \alpha \cdot \frac{\mathrm{m}}{\mathrm{e}} - \mathrm{k} \cdot \mathrm{m} + \gamma \\ \dot{\mathrm{e}} &= \beta \cdot \frac{\mathrm{k}}{\rho_{\mathrm{LDL_{ox}}}} \cdot \mathrm{m} \end{aligned} \tag{2}$$

where $\dot{\mathrm{m}}$ and $\dot{\mathrm{e}}$ are the time evolution of intimal LDL mass accumulation per unit area (m) and intimal thickness (e), respectively. The other terms of the system of equations are the density of the oxidized LDL, $\rho_{\mathrm{LDL_{ox}}} = 1060$ kg/m^3, the oxidation rate, k, the constant, β, and the parameters, α and γ, expressed in function of the physiologic variables, including the CFD-computed τ (< 0.3 Pa) and the LDL blood concentration, $\mathrm{c_{ldl}} = 1.2$ kg/m^3. The detail of parameters and further equations can be found in [10]. Moreover, a morphing procedure is applied to simulate the arterial wall thickening that allows to gradually modify the carotid geometry with a localized reduction of the lumen area normal to the arterial wall [27]. We demonstrate in [25] that τ field obtained in steady simulation are suitable to predict the plaque evolution through the model by [10]. As in [25], we choose to apply the morphing procedure every three months.

2.4 Uncertainty Quantification procedure

We carry out a stochastic sensitivity analysis to investigate the effect of the carotid geometry on the plaque onset and growth. To this aim, we build a parametric model of the carotid bifurcation (see the red lines in Fig.1). We select five parameters for the right and left carotids, viz. the ECA inflection point, the ICA inflection point, the ECA spine curvature, the ICA spline curvature, and the Reynolds number (which is related to the carotid size). The related variation ranges are reported in table 1.

We perform the analysis by using the stochastic collocation method and the sparse grid formulation. We consider an uniform Probability Density Function (PDF) for each uncertain parameter in the interval range and thus Lagrange interpolant are chosen. Clenshaw-Curtis collocation points are considered to obtain nested and bounded levels, following the progression:

$$m(i) = \begin{cases} 1, & \text{for } i = 1, \\ 2^{i-1} + 1, & \text{for } i \geq 1. \end{cases} \tag{3}$$

In our study, we use $i = 2$, resulting in a total of 61 simulations for each carotid. This

Table 1: Variation ranges of the uncertain parameters considered in the UQ procedure.

	Variation ranges	
Uncertain parameters	Right carotid	Left carotid
ECA inflection point (mm)	55-63	58.5-66.5
ICA inflection point (mm)	55.5-63.5	62-70
ECA spine curvature	0.2-1	0.8-1.6
ICA spline curvature	0.8-1.6	0.8-1.6
Reynolds	255-345	280-380

is significantly fewer than the $n^n = 5^5$ simulations required for tensor grids, allowing us to save computational resources without sacrificing accuracy. The UQ analysis is performed using the Sparse Grid Matlab Toolbox by [28]. Based on the response surface obtained through the stochastic collocation method, we employ a generalized Polynomial Chaos (gPC) expansion with Legendre polynomials to calculate the partial sensitivities σ_i.

3 RESULTS

We present the results of the stochastic sensitivity analysis for the right and left carotids, focusing on the uncertainty quantification (UQ) of plaque growth in terms of the displacement field, Δe, evaluated after one year. Figures 3 and 4 display the stochastic mean value, $\langle\Delta\text{e}\rangle$, and the stochastic standard deviation, $\sigma(\Delta\text{e})$, respectively. The plaque-onset region identified from the mean displacement field closely resembles the region found for patient-specific left and right geometries in [25], where it was determined that the LDL model provides accurate predictions for both the onset location and early-stage plaque growth. Notably, the right carotid is more prone to plaque formation throughout the bifurcation region, while in the left carotid, plaque onset and growth occur primarily on the ICA side. Significant variability in plaque growth related to local geometry is observed mainly at the plaque's edge, whereas the onset of the plaque appears independent of the local geometry.

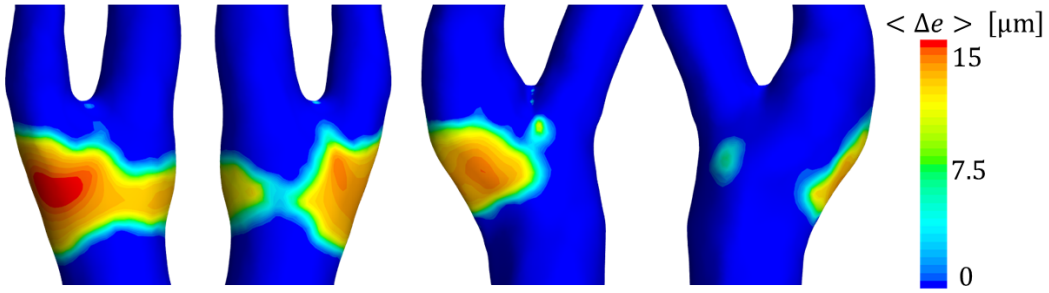

Figure 3: Stochastic mean value for the displacement field, $\langle\Delta\text{e}\rangle$, for (a) right and (b) left carotids.

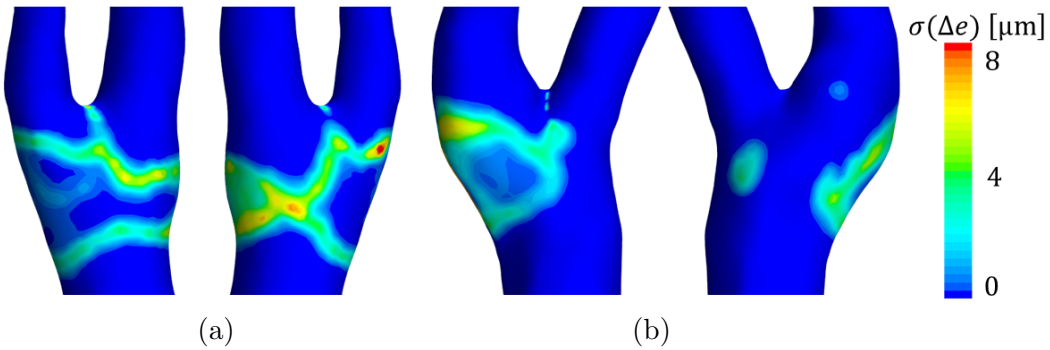

Figure 4: Stochastic standard deviation for the displacement field, $\sigma(\Delta\text{e})$, for (a) right and (b) left carotids.

The partial sensitivities of the displacement field, $\sigma_i(\Delta e)$, are shown in Fig. 5 for the right carotid and in Fig. 6 for the left carotid. For both arteries, the most significant parameter is the position of the ICA inflection point. Additionally, for the right carotid, curvature and Reynolds number are also significant factors. In contrast, plaque evolution in the left carotid is less sensitive to Reynolds number, as the plaque forms near the bifurcation, while changes in Re primarily influence wall shear stress (WSS) in the common carotid.

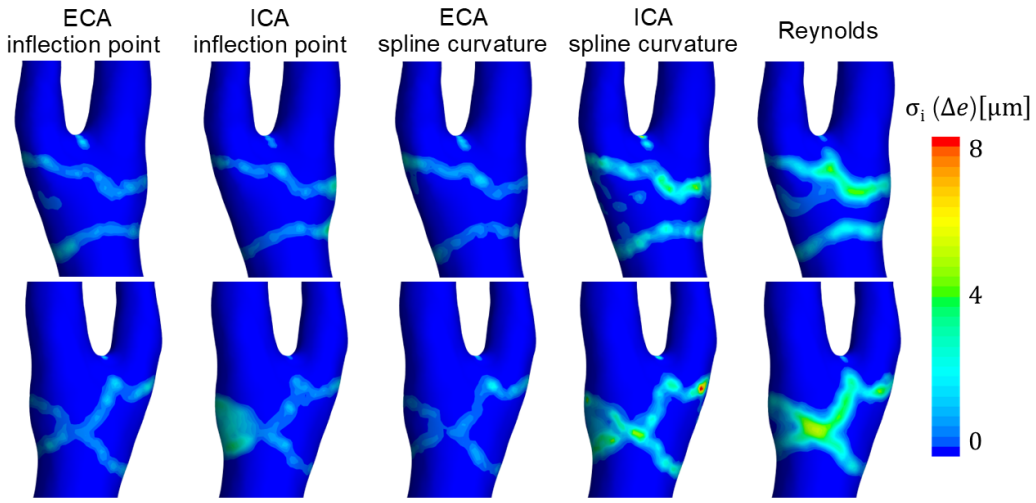

Figure 5: Partial sensitivities for the displacement field, $\sigma_i(\Delta e)$, for the right carotids.

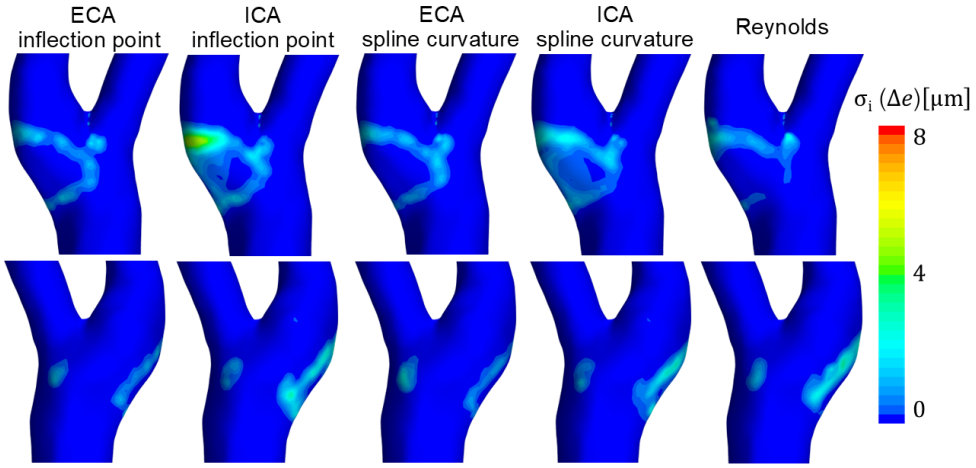

Figure 6: Partial sensitivities for the displacement field, $\sigma_i(\Delta e)$, for the left carotids.

4 CONCLUSIONS

This research focuses on evaluating the impact of hemodynamic and geometrical parameters on the potential onset and growth of atherosclerotic plaques in carotid arteries. We begin with a clinical dataset that includes patient-specific geometries and flow rates, which are used to

construct parametric models of the carotid arteries. A stochastic sensitivity analysis is then conducted using stochastic collocation methods. Plaque onset and growth are assessed through CFD simulations, integrated with the LDL-model of plaque growth from [10]. This model adapts the geometry based on the computed displacement field via a morphing procedure.

At the plaque's edge, significant variability in plaque growth is observed, closely associated with the local geometry. The most influential parameter for both carotids is the position of the ICA inflection point. Additionally, for the right carotid, curvature and Reynolds number also play a significant role.

For future work, we plan to investigate through unsteady simulations how the evolution during the cardiac cycle of the vortical structures that form at the bifurcation might help explain the results of the stochastic analysis. Furthermore, additional quantitative validation of the growth rates predicted by the numerical model, using patient-specific follow-up data, may be performed. Finally, we aim to generalize the relationship between the risk of plaque onset and growth and the geometrical parameters across more patient-specific geometries (considering not only local differences) and additional parameters, such as the inclination angle.

Acknowledgments

This research is supported by PNRR M4C2 - HPC, Big data and Quantum Computing (Simulazioni, calcolo e analisi dei dati e altre prestazioni - CN1) - CUP I53C22000690001 SPOKE 6 Multiscale modelling & Engineering applications and by the National Recovery and Resilience Plan, Mission 4 Component 2 Investment 1.3.

REFERENCES

[1] Ross, R. 1999. "Atherosclerosis—an inflammatory disease. New England journal of medicine." 340(2), 115-126.

[2] Björkegren, J.L.; Lusis, A.J. 2022. "Atherosclerosis: recent developments." Cell.

[3] Timmis, A.; Vardas, P.; Townsend, N.; Torbica, A.; Katus, H.; De Smedt, D.; Gale, C.P.; Maggioni, A.P.; Peterson, S.E.; Huculeci, R.; Kazakiewicz, R.; de Benito Rubio, V.; Ignatiuk, B.; Raisi-Estabragh, Z.; Pawlak, A.; Karagiannidis, E.; Treskes, R.; Gaita, D.; Beltrame, J.F.; McConnachie, A.; Bardinet, I.; Graham, I.; Flather, M.; Elliott, P.; Mossialos, E.A.; Weidinger, F.; Achenbach, S. 2022. "European Society of Cardiology: cardiovascular disease statistics 2021." European Heart Journal, 43(8), 716-799.

[4] Townsend, N.; Wilson, L.; Bhatnagar, P.; Wickramasinghe, K.; Rayner, M.; Nichols, M. 2016. "Cardiovascular disease in Europe: epidemiological update 2016." European heart journal, 37(42), 3232-3245.

[5] Rafieian-Kopaei, M.; Setorki, M.; Doudi, M.; Baradaran, A.; Nasri, H. 2014. "Atherosclerosis: process, indicators, risk factors and new hopes." International journal of preventive medicine, 5(8), 927.

[6] Morbiducci, U.; Gallo, D.; Massai, D.; Consolo, F.; Ponzini, R.; Antiga, L.; Bignardi, C.;Deriu, M.A.; Redaelli, A. 2010. "Outflow conditions for image-based hemodynamic mod-

els of the carotid bifurcation: implications for indicators of abnormal flow." J Biomech Eng, 132(9).

[7] Mariotti, A.; Boccadifuoco, A.; Celi, S.; Salvetti, M.V. 2021. "Hemodynamics and stresses in numerical simulations of the thoracic aorta: Stochastic sensitivity analysis to inlet flow-rate waveform." Computers and Fluids, 230, 105123.

[8] Lopes, D.; Puga, H.; Teixeira, J.; Lima, R. 2020. "Blood flow simulations in patient-specific geometries of the carotid artery: A systematic review." Journal of Biomechanics, 111, 110019.

[9] Tang, D.; Yang, C.; Mondal, S.; Liu, F.; Canton, G.; Hatsukami, T.S.; Yuan, C. 2008. "A negative correlation between human carotid atherosclerotic plaque progression and plaque wall stress: in vivo MRI-based 2D/3D FSI models." Journal of biomechanics, 41(4), 727-736.

[10] Gessaghi, V.C.; Raschi, M.A.; Tanoni, D.Y.; Perazzo, C.A.; Larreteguy, A.E. 2011. "Growth model for cholesterol accumulation in the wall of a simplified 3D geometry of the carotid bifurcation." Computer methods in applied mechanics and engineering." 200(23-24), 2117-2125.

[11] Mantzaris, M.D.; Siogkas, P.K.; Tsakanikas, V.D.; Potsika, V.T.; Pleouras, D.S.; Sakellarios, A.I.; Karagiannis, G.; Galyfos, G.; Sigala, F.; Liasis, N.; Jovanovic, N.; Koncar, I.B.; Kallmayer, M.; Fotiadis, D.I. 2021. "Computational modeling of atherosclerotic plaque progression in carotid lesions with moderate degree of stenosis." In 2021 43rd Annual International Conference of the IEEE Engineering in Medicine and Biology Society (EMBC), (pp. 4209-4212). IEEE.

[12] Alagbe, E.E.; Amoo, T.E.; Ayeni, A.O.; Oyedele, O.S.; Ashiekaa, V.D. 2022. "Computational Simulation of Atherosclerosis Progression Associated with Blood Pressure in a 2-D Idealized Human Carotid Artery Model." The Open Chemical Engineering Journal, 16(1).

[13] Holdsworth, D.W.; Norley, C.J.D.; Frayne, R.; Steinman, D.A.; Rutt, B.K. 1999. "Characterization of common carotid artery blood-flow waveforms in normal human subjects." Physiological measurement, 20(3), 219.

[14] Mariotti, A.; Vignali, E.; Gasparotti, E.; Morello, M.; Singh J.; Salvetti, M.V.; Celi, S. 2023. "In Vitro Analysis of Hemodynamics in the Ascending Thoracic Aorta: Sensitivity to the Experimental Setup." Applied Sciences (Switzerland), 13(8), 5095.

[15] Mirbagheri, S.A.; Saidi, M.S.; Sohrabi, S.; Firoozabadi, B.; Banazadeh, M.H. 2016. "Effects of hypertension on Intima-Media Thickness (IMT); application to a human carotid artery." Scientia Iranica, 23(4), 1731-1740.

[16] Mendieta, J.B.; Fontanarosa, D.; Wang, J.; Paritala, P.K.; McGahan, T.; Lloyd, T.; Li, Z. 2020. "The importance of blood rheology in patient-specific computational fluid dynamics simulation of stenotic carotid arteries." Biomechanics and Modeling in Mechanobiology, 19, 1477-1490.

[17] Weddell, J.C.; Kwack, J.; Imoukhuede, P.I.; Masud, A. 2015. "Hemodynamic analysis in an idealized artery tree: differences in wall shear stress between Newtonian and non-Newtonian blood models." PloS one, 10(4), e0124575.

[18] Morbiducci, U.; Gallo, D.; Massai, D.; Ponzini, R.; Deriu, M. A.; Antiga, L.; Montevecchi, F.M. 2011. "On the importance of blood rheology for bulk flow in hemodynamic models of the carotid bifurcation." Journal of biomechanics, 44(13), 2427-2438.

[19] Spanos, K.; Petrocheilou, G.; Karathanos, C.; Labropoulos, N.; Mikhailidis, D.; Giannoukas, A. 2017. "Carotid bifurcation geometry and atherosclerosis." Angiology, 68(9), 757-764.

[20] Morbiducci, U.; Kok, A.M.; Kwak, B.R.; Stone, P.H.; Steinman, D.A.; Wentzel, J.J. 2016. "Atherosclerosis at arterial bifurcations: evidence for the role of haemodynamics and geometry." Thrombosis and haemostasis, 115(03), 484-492

[21] Ninos, G., Bartzis, V., Merlemis, N., & Sarris, I. E. 2021. "Uncertainty quantification implementations in human hemodynamic flows." Computer Methods and Programs in Biomedicine, 203, 106021.

[22] Perktold, K.; Resch, M. 1990. "Numerical flow studies in human carotid artery bifurcations: basic discussion of the geometric factor in atherogenesis." Journal of Biomedical Engineering, 12(2), 111-123.

[23] Lee, S.W.; Antiga, L.; Spence, J.D.; Steinman, D.A. 2008. "Geometry of the carotid bifurcation predicts its exposure to disturbed flow." Stroke, 39(8), 2341-2347.

[24] Sankaran, S., & Marsden, A. L. 2011. "A stochastic collocation method for uncertainty quantification and propagation in cardiovascular simulations." J Biomech Eng., 133(3): 031001 (12 pages).

[25] Singh, J.; Capellini, K.; Mariotti, A.; Salvetti, M.V.; Celi, S. 2024. "Predicting atherosclerotic plaque onset and growth in carotid arteries: a CFD-driven approach." in: I. Rojas et al. (Eds.): IWBBIO 2024, LNBI 14848, pp. 1–12, 2024.

[26] Marshall, I.; Papathanasopoulou, P.; Wartolowska, K. 2004. "Carotid flow rates and flow division at the bifurcation in healthy volunteers." Physiological measurement, 25(3), 691.

[27] Capellini, K.; Gasparotti, E.; Cella, U.; Costa, E.; Fanni, B.M.; Groth, C.; Porziani, S.; Biancolini, M.E.; Celi, S. 2021. "A novel formulation for the study of the ascending aortic fluid dynamics with in vivo data." Medical Engineering & Physics, 91, 68-78.

[28] Piazzola, C. and Tamellini, L. 2022. "The Sparse Grids Matlab kit - a Matlab implementation of sparse grids for high- dimensional function approximation and uncertainty quantification."

[29] Homma, S.; Hirose, N.; Ishida, H.; Ishii, T.; Araki, G. 2001. "Carotid plaque and intima-media thickness assessed by b-mode ultrasonography in subjects ranging from young adults to centenarians." Stroke, 32(4), 830-835.